Designing analysis of the polarization beam splitter in two communication bands based on a gold-filled dual-core photonic crystal fiber*

Fan Zhen-Kai(范振凯), Li Shu-Guang(李曙光)†, Fan Yu-Qiu(范玉秋), Zhang Wan(张 婉), An Guo-Wen(安国文), and Bao Ya-Jie(鲍亚杰)

Key Laboratory of Metastable Materials Science and Technology, College of Science, Yanshan University, Qinhuangdao 066004, *China*

(Received 11 December 2013; revised manuscript received 26 March 2014; published online 23 July 2014)

We design a novel kind of polarization beam splitter based on a gold-filled dual-core photonic crystal fiber (DC-PCF). Owing to filling with two gold wires in this DC-PCF, its coupling characteristics can be changed greatly by the second-order surface plasmon polariton (SPP) and the resonant coupling between the surface plasmon modes and the fiber-core guided modes can enhance the directional power transfer in the two fiber-cores. Numerical results by using the finite element method show the extinction ratio at the wavethlengths of 1.327 μm and 1.55 μm can reach −58 dB and −60 dB and the bandwidths as the extinction ratio better than −12 dB are about 54 nm and 47 nm, respectively. Compared with the gold-unfilled DC-PCF, a 1.746-mm-long gold-filled DC-PCF is better applied to the polarization beam splitter in the two communication bands of $\lambda = 1.327$ μm and 1.55 μm.

Keywords: photonic crystal fiber, polarization beam splitter, surface plasmon

PACS: 42.81.−i, 42.81.Pa, 71.45.Gm **DOI:** 10.1088/1674-1056/23/9/094212

1. Introduction

Photonic crystal fibers have some new applications, such as a polarization beam splitter (PBS),[1–3] optical sensor,[4–6] and optical coupler.[7–9] Especially, the polarization beam splitter has caused widespread concern in communication in recent years.[8–10] A wide variety of polarization beam splitters have been reported in journals. For example, Zhang and Yang designed a new polarization beam splitter based on DC-PCF, of which the extinction ratio is better at −11 dB with a bandwidth of 40 nm.[10] Liu *et al.* reported a 0.36-mm-long polarization beam splitter, whose bandwidth with the extinction ratio is better than −10 dB is 20 nm.[11]

An extended metal gold interface can sustain propagating electromagnetic waves that are coupled to collective oscillations of the conduction electrons in gold, so called surface plasmon polaritons (SPPs). Some experimental methods have been proposed by blocking selected holes of photonic crystal fibers and filling them with liquid gold. The micron sized wires are able to be introduced into silica fibers.[12] Numerical simulation shows that the surface plasmon polariton (SPP) is able to transmit the directional power from one core to another core.[13] For example, Zhang *et al.* analyzed the polarization coupling characteristics of a new structure of dual-core photonic crystal fiber filled with metal wire in the cladding air hole, and the extinction ratio is better: 30.54 dB at the wavelength of 1.550 μm.[14] Sun *et al.* proposed the polarization beam splitter whose the extinction ratio is as low as −20 dB with a bandwidth as great as 146 nm.[15] Recently, Li *et al.* numerically investigated the polarization-dependent coupling in DC-PCF selectively filled with gold wires in air holes. Above all, the study suggests that a gold-filled DC-PCF is a new possibility for applications on polarization beam splitters.

In this paper, we design a novel polarization beam splitter in two communication bands based on a gold-filled DC-PCF. Numerical simulations with the finite element method show the dispersion and loss of the gold-filled DC-PCF are strongly effected by the second-order SPP. Compared with the gold-unfilled DC-PCF, the gold-filled DC-PCF has a shorter coupling length and a lower extinction ratio at the wavelengths of 1.327 μm and 1.55 μm. At the same time, the bandwidth has an extinction better than −12 dB, which is much wider than that of the gold-unfilled DC-PCF. Thus, our results certify that the gold-filled DC-PCF can be better applied in the polarization beam splitter at the wavelengths of 1.327 μm and 1.55 μm.

2. New structure and the fundamental theory

The schematic cross-section of the gold-filled DC-PCF is shown in Fig. 1. The cladding holes have been arranged in a triangular lattice in a pure silica background and the parameters of the fiber are as follows:the diameter of $d = 1$ μm and the lattice constant $\Lambda = 2.0$ μm. Furthermore, all the gray circles represent the air holes, and the cores of A and B are obtained by removing two air holes and the two black holes in the near A and B are replaced by two gold wires in the x-polarization direction. The modal birefringence can be increased through

*Project supported by the National Natural Science Foundation of China (Grant Nos. 61178026) and the Natural Science Foundation of Hebei Province, China (Grant No. E2012203035).

†Corresponding author. E-mail: shuguangli@ysu.edu.cn

© 2014 Chinese Physical Society and IOP Publishing Ltd

filling two gold wires in the fiber. Besides, the error about the numerical simulation is caused by the material dispersion, which is calculated by the Sellmeier equation. The refractive index of air is considered as 1. The permittivity of the gold wire has been calculated by a more accurate Drude–Lorentz model,[16–18] and the equation can be shown as follows:

$$\varepsilon_{\mathrm{m}} = \varepsilon_{\infty} - \frac{\omega_{\mathrm{D}}^2}{\omega(\omega + \mathrm{j}\gamma_{\mathrm{D}})} - \frac{\Delta\varepsilon \cdot \Omega_{\mathrm{L}}^2}{(\omega^2 - \Omega_{\mathrm{L}}^2) + \mathrm{j}\Gamma_{\mathrm{L}}\omega}, \tag{1}$$

where the values and physical meaning of ε_{∞}, ω_{D}, γ_{D}, Ω_{L}, and Γ_{L} can be achieved in Ref. [19]. Values of the optimized parameters have fitted the experimental data of bulk gold. The complex propagation constants of the waveguide modes can be calculated by using the finite-element method, and the confinement loss can be precisely estimated by adding the perfectly matched layer (PML).[20–22]

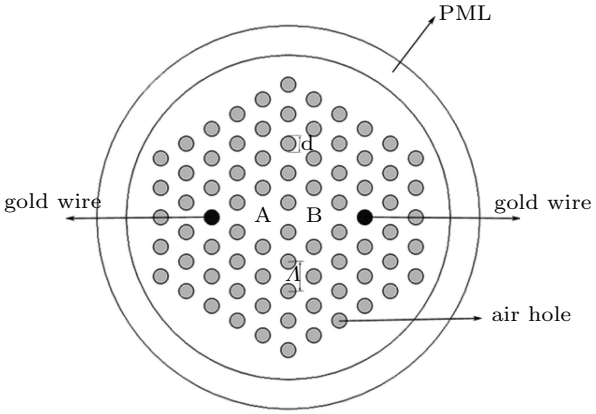


Fig. 1. Schematic diagram of the gold-filled dual-core photonic crystal fiber. The two black circles represent two gold wires. The rest of the gray circles represent the air holes, and the alphabet A and B represent two cores of the DC-PCF. A perfectly matched layer (PML) with several micrometers is added to the outmost layer, which is used for absorbing the radiation energy.

The designed polarization beam splitter can be analyzed by using the coupled mode theory. When a beam light is launched into one core of the gold-filled DC-PCF, the *x*- and *y*-polarization modes of this beam light can be separated through the suitable distance during transmission. Further consideration, the coupling characteristics of the polarization beam splitter can be obtained by calculating the effective refractive indices of the *x*, *y*-polarized even and odd modes. The coupling length of the *x*- and *y*-polarized modes is calculated through the equation:[23–25]

$$L^{x,y} = \frac{\lambda}{2(n_{\mathrm{even}}^{x,y} - n_{\mathrm{odd}}^{x,y})}, \tag{2}$$

where $n_{\mathrm{even}}^{x,y}$ and $n_{\mathrm{odd}}^{x,y}$ are the real part of the effective index of the *x* and *y*-polarized even and odd modes, and the units of the coupling length and wavelength are micrometers.

The normalized power and extinction ratio are the key parameters of the polarization beam splitter, which are able to measure the spectral properties of the splitter. As the two cores of A and B are identical, the energy will transfer from one core into the other core and back again along the fiber. The normalized power can be calculated as:[26,27]

$$P_{\mathrm{out}}^{x,y} = P_{\mathrm{in}}^{x,y} \cos\left(\frac{\pi Z}{2L}\right). \tag{3}$$

Extinction ratio (ER) is defined as the power of a particular polarization in the expected output core compared to the power of the other polarization in the same core. The ER of the polarization beam splitter can be calculated as follows:[28–30]

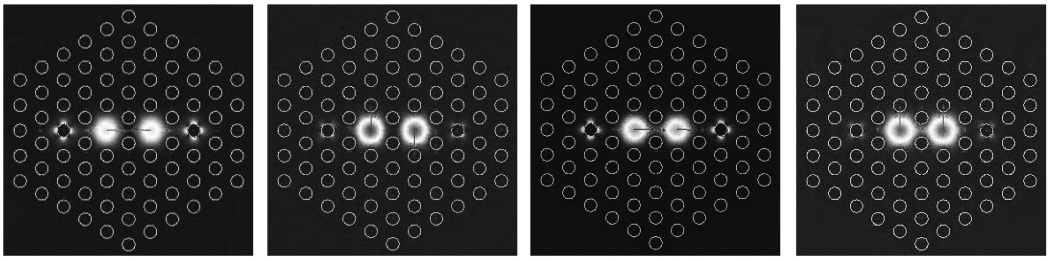
$$\mathrm{ER} = 10\lg\frac{P_{\mathrm{out}}^{x}}{P_{\mathrm{out}}^{y}}, \tag{4}$$

where $P_{\mathrm{in}}^{x,y}$ and $P_{\mathrm{out}}^{x,y}$ represent the input and output powers of the *x*- and *y*-polarized modes of the polarization beam splitter, respectively.

3. Characteristics of the gold-filled DC-PCF

3.1. Resonance coupling modes

We present first an insight into all kinds of resonance coupling modes of the gold-filled DC-PCF in Fig. 2. Numerical analysis certified that a wavelength selection characteristic is produced by the resonance coupling between four kinds of core-guided modes and the surface plasmon modes. Furthermore, the resonance coupling between the *x*- and *y*-odd modes (Figs. 2(a) and 2(b)) and the second-order SPP mode can be obtained at the wavelength of 1.170 μm, and the *x*- and *y*-even modes (Figs. 2(c) and 2(d)) with the second-order SPP mode can resonate at the wavelength of 1.160 μm. It is observed that the resonance of the *x*-polarized direction is more obvious than the *y*-direction.



(a) (b) (c) (d)

Fig. 2. Power flow distributions of the resonance coupling modes in this DC-PCF. Panels (a)–(d) represent the *x*-odd mode, *y*-odd mode, *x*-even mode, and *y*-even mode, respectively.

3.2. Dispersion and loss of the gold-filled DC-PCF

Figures 3(a) and 3(b) show the schematic illustration of the gold-filled DC-PCF dispersion relation of the *x*- and *y*-polarized modes, respectively. The resonance coupling between the four core-guided modes and 2nd or 3rd order SPP modes can emerge in the wavelength from 0.8 μm to 1.6 μm. We can discover the obvious gaps of the effective refractive index of the even and odd mode in the *x*- and *y*-polarized directions, respectively. When the effective refractive indices between the SPP modes and the core-guided modes are matching, the resonance coupling will reach to the strongest. Therefore, it is found that the 2nd SPP modes and the *x*, *y*-even modes or the *x*, *y*-odd modes meet the phase matching condition at the vicinity of the anti-crossing point about 1.170 μm or 1.160 μm. Similarly, the 3rd SPP modes with *x*- and *y*-polarized core-guided modes can meet the phase matching condition at the resonance wavelength about 0.823 μm and 0.825 μm. In the research, the effective refractive index of the first SPP mode is much higher than that of the core-guided modes, so that it is quite difficult for the resonance coupling from the SPP modes to the core-mode.

In the following sections, figures 4(a) and 4(b) show the loss of the *x*- and *y*-polarized modes, respectively. Apparently, it is observed that the loss of the *x*- and *y*-polarized modes can reach to the peak at the resonance wavelength where the core-guided mode and the SPP mode are crossing. As the resonance coupling of the *x*-polarized modes is much stronger than that of the *y*-polarized modes, the loss of *x*-polarized modes is much higher than that of the *y*-polarized modes. Besides, the resonance *w* of the *x*- or *y*-even modes and the 2nd-order SPP modes is at the wavelength of 1160 nm, that of the *x*- and *y*-odd modes is at the wavelength of 1170 nm, respectively. The loss of *x*- and *y*-even modes can reach to 145 dB/cm and 58 dB/cm, and the *x*-and *y*-odd modes loss can reach to 262 dB/cm and 24 dB/cm, respectively. Those results indicate that the loss of four core-modes can be obviously excited to the peak when the SPP modes and core-guided modes meet phase matching condition. However, the difference of the effective refractive indices in *x*-even and *x*-odd modes is much greater than that of the *y*-polarized one, which will greatly change the coupling characteristic between two core-guided modes. This new discovery can be applied to polarization beam splitters.

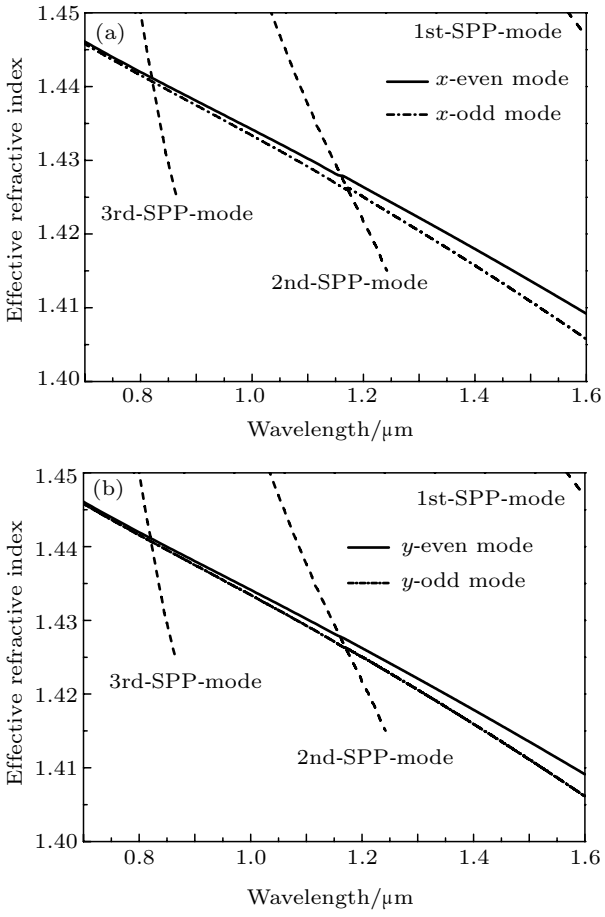


Fig. 3. The wavelength dependence of the effective refractive index. Panel (a) shows the effective refractive index of the *x*-even and odd modes with the solid and dash dotted curves, respectively. Panel (b) shows that of the *y*-even and odd modes with the solid and short dashed curve, respectively. All SPP modes are expressed by the dotted curves.

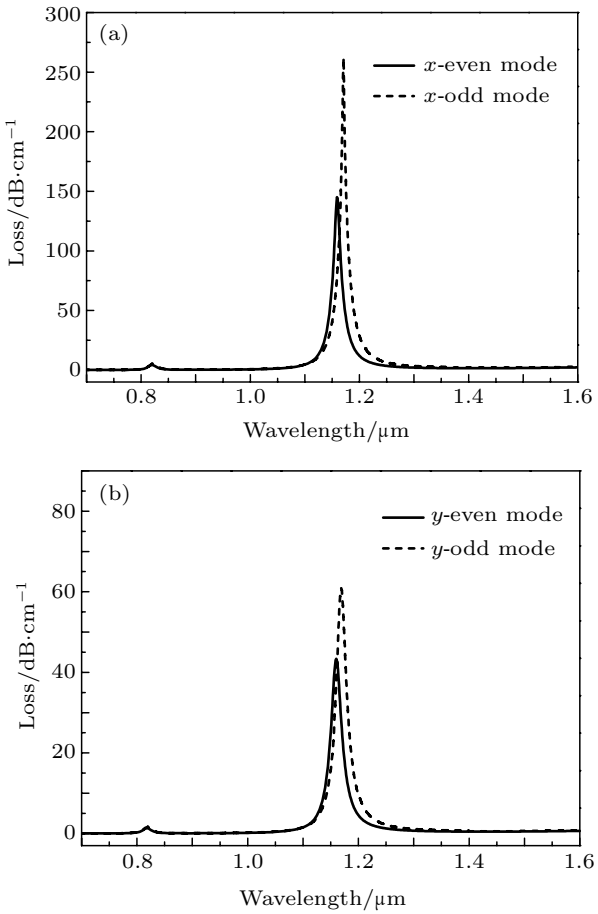


Fig. 4. The wavelength dependence of the loss on the *x*- and *y*-polarized modes. The solid lines of panels (a) and (b) depict the loss of the *x*- and *y*-polarized even modes, and the dashed lines of that represent the loss of the *x*- and *y*-polarized odd modes, respectively.

3.3. Polarization beam splitter

Figure 5 shows the wavelength dependence of the coupling length of the x- and y-polarized modes on the gold-filled and the gold-unfilled DC-PCF. As the value of $\mathrm{Re}[n_{\mathrm{even}}^{x,y} - n_{\mathrm{odd}}^{x,y}]$ for the gold-filled DC-PCF is much larger than that for the gold-unfilled DC-PCF, the coupling length of the gold-filled DC-PCF is decreased by Eq. (2). Thus it is obvious that the coupling characteristic of the x- and y-polarized modes can be significantly affected by the two gold wires. The coupling length of the x- and y-polarized modes for the gold-filled DC-PCF can reach 245 μm and 288 μm at the wavelengths of $\lambda = 1.327$ μm and 1.55 μm, and that of the gold-unfilled DC-PCF are 255 μm and 299 μm, respectively.

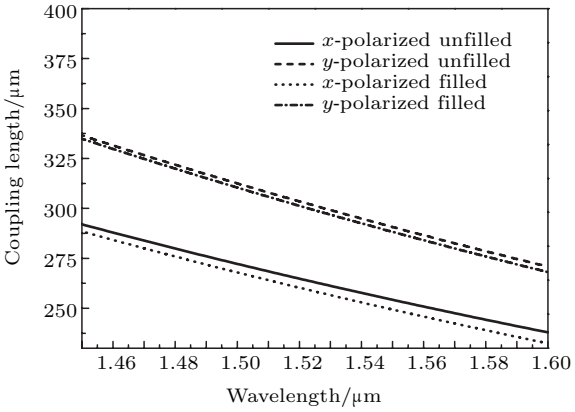


Fig. 5. The wavelength dependence of the coupling length on the gold-unfilled and gold-filled DC-PCF. The solid and dashed curves represent the x- and y-polarized coupling length of the unfilled DC-PCF, and the dotted and dash dotted curves express that of the gold-filled DC-PCF, respectively.

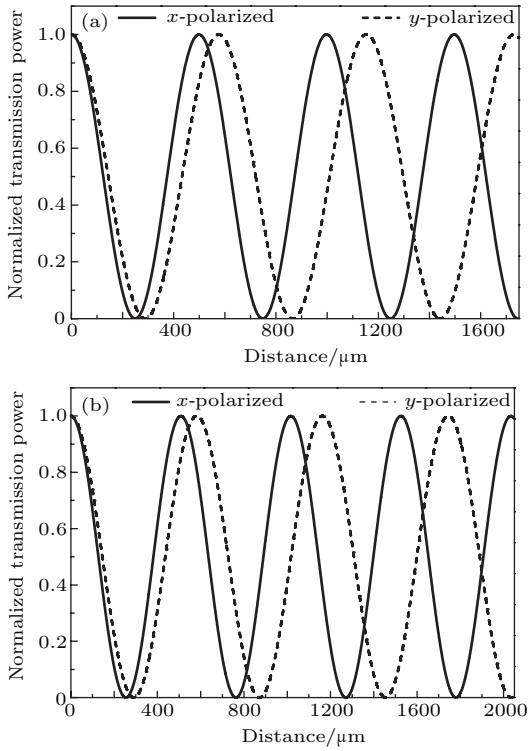


Fig. 6. The normalized transmission power of the filled-gold (a) and unfilled-gold (b) DC-PCF as the changing distance at the wavelength of 1.55 μm. Besides, the solid lines and the dashed lines denote the normalized powers of the x- and y-polarized modes, respectively.

Figure 6 shows the normalized power as a function of the transmission distance. Figure 6(a) demonstrates that the gold-filled DC-PCF can be applied for the polarization beam splitter at the wavelength of 1.55 μm. When the transmission distance is $z = 7L_x = 6L_y = 1.746$ mm. Figure 6(b) shows the unfilled DC-PCF can be used for the polarization beam splitter at the wavelength of 1.55 μm, when the transmission distance is $z = 8L_x = 7L_y = 2.035$ mm. When a beam of light launches into the A-core of the gold-filled DC-PCF, the x-polarized mode can couple into the B-core, while the y-polarized mode cannot couple into the B-core at the distance of 1.746 mm. For the unfilled DC-PCF, the x-polarized mode cannot couple into the B-core, while the y-polarized mode can couple into the B-core at the distance of 2.035 mm.

Figure 7 shows the normalized transmission power as the changing of wavelength (from 1.2 μm to 1.6 μm) for the gold-filled and unfilled DC-PCF. We can discover the cyclical change of the normalized transmission powers with the increasing of wavelength. Figures 7(a) and 7(b) illustrate that the normalized transmission powers of the x- and y-polarized modes can be separated into two fiber-cores for the filled-gold and unfilled-gold DC-PCF at the wavelength of 1.55 μm, respectively.

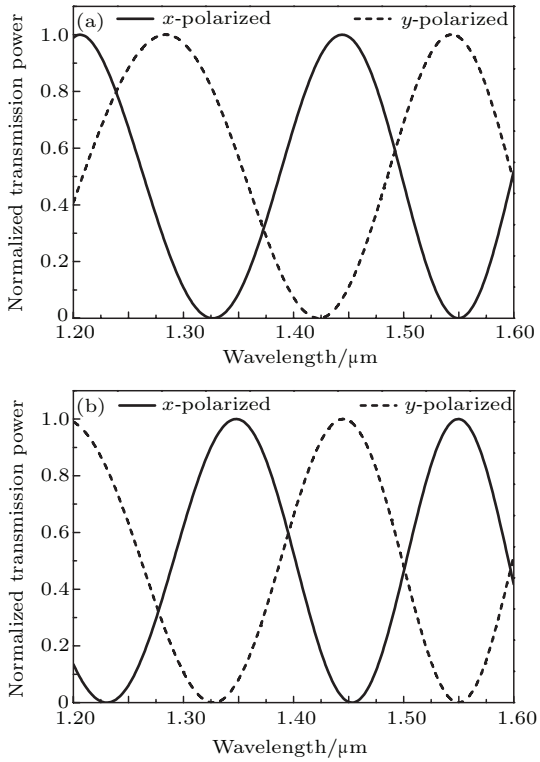


Fig. 7. The normalized transmission power of the gold-filled (a) and unfilled DC-PCF (b) with the variation of the wavelength from 1.2 μm to 1.6 μm. The solid lines and the dashed lines represent the x- and y-polarized normalized transmission powers, respectively.

Figure 8 shows the wavelength dependence of ER on the gold-filled and unfilled DC-PCF. From Fig. 8(a), we can see the extinction ratio is better than −12 dB at the wavelengths

of near 1.327 μm and 1.55 μm, and the bandwidths are 54 nm and 47 nm, respetively. At the wavelengths of 1.327 μm and 1.55 μm, the extinction ratios can reach to −58 dB and −60 dB. Figure 8(b) shows the extinction ratio is better than 10 dB at the wavelengths of near 1.327 μm and 1.55 μm with the bandwidths of 40 nm and 32 nm, and the extinction ratios are able to reach to 40 dB and 45 dB at the two wavelength points of $\lambda = 1.327$ μm and $\lambda = 1.55$ μm, respectively. Compared with the unfilled DC-PCF, the gold-filled DC-PCF has a much higher the extinction ratio and the wider bandwidth in two communication bands of 1.327 μm and 1.55 μm, which will be better applied to the polarization beam splitter.

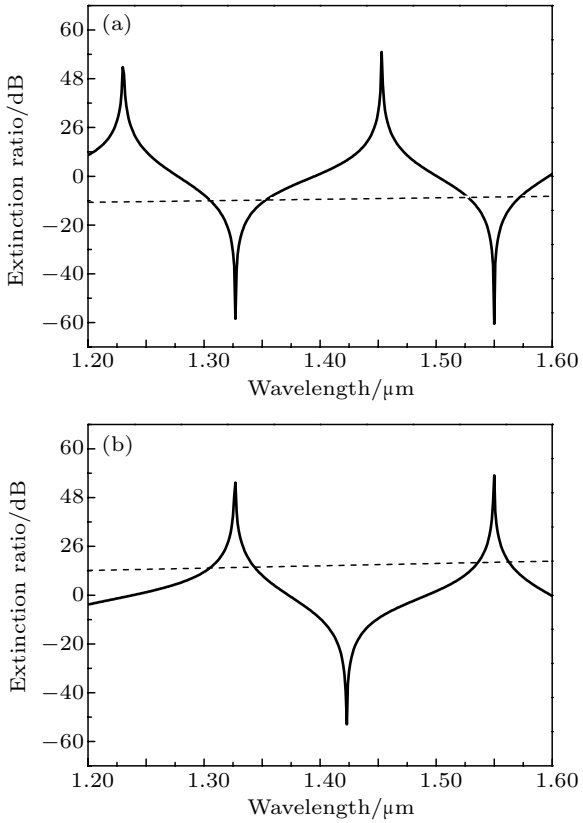


Fig. 8. The wavelength dependence of the extinction ratio on the gold-filled (a) and gold-unfilled (b) DC-PCF. The dashed lines of panels (a) and (b) represent the extinction ratio values of −12 dB and 10 dB, respectively.

4. Conclusions

We proposed a novel kind of polarization beam splitter based on the gold-filled DC-PCF in this paper. The dispersion of the *x*- and *y*-polarized modes can be effected greatly by the second-order SPP. The resonant wavelength of the even and odd modes for the *x*- and *y*-polarized modes appear in different positions, and the resonance strength of *x*-polarized modes is much stronger than that of *y*-polarized modes. In addition, the coupling lengths of the *x*- and *y*-polarized modes are reduced by the enhanced birefringence in the fiber. Numerical simulations certify that a 1.746-mm-long fiber can ensure a split of the *x*- and *y*-polarized modes into two cores at the wavelengths of 1.327 μm and 1.55 μm, whose the extinction ratios can reach to the lowest −58 dB and −60 dB, and the bandwidths with an extinction ratio better than −12 dB are 54 nm and 47 nm, respectively. Furthermore, the splitter with a symmetric structure is much easier to be fabricated by using a drawn tower. We believe this novel type of splitter will be useful in future optical communication systems, especially for fiber-to-the-home applications.

References

[1] Liu S, Li S G, Ying G B and Wang X D 2012 *Chin. Phys. B* **21** 034217
[2] Saitoh K, Sato Y and Koshiba M 2004 *Opt. Express* **12** 3940
[3] Liu S, Li S G, Ying G B and Wang X D 2011 *Opt. Commun.* **285** 1097
[4] Qin W, Li S G, Xue J R, Xin X J and Zhang L 2013 *Chin. Phys. B* **22** 074213
[5] Xie Z G, Lu Y H, Wang P, Lin K Q, Yan J and Ming H 2008 *Chin. Phys. Lett.* **25** 4473
[6] Gauvreau B, Hassani A and Fassi F M 2007 *Opt. Express* **15** 11413
[7] Li P and Zhao J L 2012 *Opt. Express* **21** 52329
[8] Yan F P, Wang L, Mao X Q, Gong T R, Liu P, Tao P L and Peng W J 2010 *Opt. Commun.* **283** 3658
[9] Yan F P, Li Y F, Wang L, Gong T R, Liu P, Liu Y, Tao P L, Qu M X and Jian S S 2008 *Acta Phys. Sin.* **57** 5735 (in Chinese)
[10] Zhang L and Yang C X 2003 *Opt. Express* **11** 1015
[11] Liu S, Li S G and Du Y 2012 *Opt. Laser Technol.* **44** 1813
[12] Lu Y, Hao C J, Wu B Q, Musideke M, Duan L C, Wen W Q and Yao J Q 2013 *J. Sens.* **13** 956
[13] Du Y, Li S G, and Liu S 2012 *Chin. Phys. B* **21** 094219
[14] Zhang S Y, Yu X, Zhang Y, Shum P, Zhang Y T, Xia L and Liu D M 2012 *IEEE Photon. J.* **1** 265
[15] Sun B, Chen M Y, Zhou J and Zhang Y K 2013 *Plasmonics* **8** 1253
[16] Zhang Z X, Hu M L, Chan T K and Wang C Y 2010 *Opt. Lett.* **35** 3091
[17] Chen W Q, Thoreson M D, Ishii S, Kildishev A V and Shalaev V M 2010 *Opt. Express* **18** 5124
[18] Laroche A V T 2008 *Appl. Phys. B* **93** 139
[19] Hao F and Nordlander P 2007 *Chem. Phys. Lett.* **446** 115
[20] Nagasaki A, Saitoh K and Koshib M 2008 *Opt. Express* **19** 3800
[21] Xue J R, Li S G, Xiao Y Z, Qin W, Xin X J and Zhu X P 2013 *Opt. Express* **21** 13733
[22] Zhou C, Zhang Y T, Xia L and Liu D M 2012 *Opt. Commun.* **285** 2466
[23] Wang Z, Taru T, Birks T A, Knight J C, Liu Y and Du J 2007 *Opt. Express* **15** 4795
[24] Hameed M F O, Obayya S S A, Begain K A, Nasr A M and Aboel Maaty M I 2011 *Iet. Opt.* **3** 264
[25] Chen M Y, Sun B, Zhang Y K and Fu X X 2010 *Appl. Opt.* **49** 3042
[26] Li J F, Duan K L, Wang Y S, Cao X J, Guo Y K and Lin X D 2009 *Optik* **120** 490
[27] Li S S, Zhang H, Hou Y, Bai J J, Liu W W and Chang S J 2013 *Appl. Opt.* **52** 3305
[28] Chow K K, Shu C and Lin C L 2005 *Opt. Express* **13** 8900
[29] Zhang S S, Zhang W G, Geng P C, Li X L and Ruan J 2011 *Appl. Opt.* **50** 6576
[30] Lu W L, Lou S Q, Wang X, Wang L W and Feng R J 2012 *Appl. Opt.* **52** 449